European Journal of Business & Social Sciences
Available at https://ejbss.org/

ISSN: 2235-767X
Volume 07 Issue 04
April 2019

Photothermal Beam Deflection Technique for Optoelectronic Properties of Semiconductor Thin Films

Shamim Akhtar[1], Dr. Mohan Nathulal Giriya

[1]Research Scholar, Department of Physics, Sri Satya Sai University of Technology & Medical Sciences, Sehore, MP(India)

ABSTRACT

Nonradiative transitions occurring in semiconductors result in thermal emissions carrying information on the material's thermal and electronic properties. A simple one-dimensional theoretical model is devised which accounts for the photothermal signal variations due to nonradiative transitions occurring in semiconductor thin films. The theory was verified by determining the transport properties of p-type silicon wafer. We could get the thermal diffusivity, minority carrier lifetime, surface recombination velocity, and minority carrier mobility of $CuInS_2$ thin films, thereby proving the efficiency and simplicity of photothermal beam deflection technique for real time characterization of semiconductor thin films.

KEYWORDS: Non-destructive testing, Copper indium disulphide, Photothermal beam deflection

1.1 INTRODUCTION

Non-destructive testing (NDT) is the process of evaluating a material, component or system without causing any loss or damage to the material under study. Non-destructive evaluation of a material guarantees its cost effectiveness, reliability and safety of operation. It also assists to avoid failures, control of manufacturing process and maintain the product quality level. Photothermal (PT) techniques offers a huge range of methods by which the materials can be evaluated non-destructively. Photothermal techniques for thermal NDT measurements were first developed around 1980 and have ever since been in use for a huge range of spectroscopic and imaging applications. It is a growing technique in the NDT field and for actual field application.

"Mirage effect" or Photothermal beam deflection (PTBD) phenomenon deals with bending of a light beam due to the thermal gradient in the medium through which it travels. Due to lack of satisfactory theoretical explanations, this effect remained dormant for a long period without any commendable application. A strict mathematical interpretation of thermal wave propagation in solids is essential to give a good theoretical explanation of the experimental results observed using photothermal phenomenon and for the retrieval of the necessary information related to material properties. The interest in this area was revived by Rosencwaig et al [1], which resulted in the development of 'photoacoustic' technique for spectroscopic investigation of solid and semisolid materials. This theoretical model gave sufficient explanation for generation and propagation of thermal wave and this led to the boom of several photothermal detection techniques with wide spread applications.

European Journal of Business & Social Sciences
Available at https://ejbss.org/
ISSN: 2235-767X
Volume 07 Issue 04
April 2019

Transverse PTBD technique, in skimming configuration, where the probe beam propagates perpendicular to the pump beam and at a fixed distance from the sample surface, has been widely studied by several groups [2-5] since past three decades.

Photothermal effect in solids

Primary source of photothermal signal arises due to the periodic heat flow from solid to its surrounding as the solid is heated using a modulated light. Only a relatively thin layer of medium (0. 2 cm for a chopping rate of 100 Hz) adjacent to the surface of the solid responds thermally to the periodic heat flow from the solid. This is a diffusive process that produces a periodic temperature distribution and the amplitude of the signal thus generated depends on the quantity of the heat emanating from the illuminated sample; there is a close correspondence between the strength of the signal and the amount of light absorbed.
Photothermal signal amplitude also depends on the sample's overall light absorption irrespective of whether it is volume or surface related. On other hand, photothermal phase signal depends also on the localization of the absorption. In fact, in an absorbing sample, the light absorbed in part or in the entire sample volume acts as an effective centre of heating source, whose position depends on the sample optical absorption depth, ($\mu b=1/b$) of the sample and thermal diffusion length, ($\mu = 1/a$). Farther the position of this centre from the sample front surface, the greater will be the phase lag (the smaller the phase value) with respect to a reference signal. When the bulk absorption only is involved, the centre of the source will be located somewhere in the sample volume and this will correspond to a definite phase value. If surface states are also present on the sample front or rear surface or even buried within the sample volume, position of the "centre" shifts towards the absorbing layer and the phase value will correspondingly change. From a simultaneous analysis of both the photothermal signal amplitude and phase, it is possible to locate the eventual presence of surface states and to measure their absorption.

Photothermal effect in semiconductors

When a semiconductor material is illuminated with photons of sufficient energy, electron-hole pairs are generated which diffuse through the crystal from their place of generation to regions of lower excess pair concentration. Each pair transports energy approximately equal to the band separation, thus contributing to the thermal conductivity. This energy is deposited where the pair undergoes non-radiative recombination increasing the local measurable temperature of the lattice. A non-uniform temperature distribution is therefore established in the sample which depends on the nature of the incident radiation, on the characteristics of optical absorption, on the boundary conditions for temperature and energy flux, and on the ordinary thermal conductivity of the material. Thus, establishment of a temperature distribution in a solid by optical excitation, diffusion and recombination of carriers and the attendant modification in thermal conductivity is called "photothermal effect".

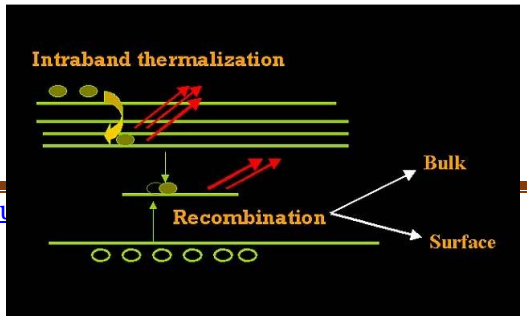

European Journal of Business & Social Sciences
Available at https://ejbss.org/
ISSN: 2235-767X
Volume 07 Issue 04
April 2019

Figure 1.1 Photothermal effect in semiconductors

1.2 THEORETICAL APPROACH

Photothermal beam deflection theory shows that the transverse deflection from the original trajectory of the probe beam depends on the thermal gradients in the direction orthogonal to the path only according to the well-known formula, which, in geometric optics, is written as,

$$\Phi = \frac{1}{n_{air}}\left(\frac{dn_{air}}{dT}\right)\int_{path}\Delta_t T_{air}\left(x,y,z\right)ds \quad \ldots\ldots\ldots\ldots\ldots\ldots\ldots\ldots(1.1)$$

Where n_{air}, dn_{air}/dT represent the air refractive index and the optothermal parameter respectively, T_{air} is the temperature rise in air, and Δ_t is the gradient transverse to the probe paths.

A one-dimensional model of heat flow in the cell resulting from the absorbed light energy was put forth by Rosencwaig et al [1] for measuring the signal generated in photoacoustic technique. Later in 1990, U Zammit et al [10] developed a 1-D theoretical model for analysis of photothermal deflection signal amplitude and phase. According to this theory any light absorbed by the solid is converted, in part or whole, into heat by non-radiative deexcitation processes within the solid. The general 1-D expression for deflection signal [S] for a compact photothermal defection spectroscopy assembly with CCl_4 as coupling medium is given by,

$$S = T_r = \left(\frac{1}{n_0}\right)\frac{dn}{dT}l\frac{dT\left(Z_0\right)}{dz}e^{iax} \quad \ldots\ldots\ldots\ldots\ldots\ldots\ldots\ldots\ldots\ldots\ldots..(1.2)$$

Where T_r is the transducer factor, $(1/n_0)(dn/dT)$ is the relative index of refraction change with temperature of the deflecting medium, l is the interaction length, z_0 is the distance of the probe beam from the sample surface, and $T\left(z\right)=T_0e^{-\sigma mz}$ is the ac temperature rise above the average temperature in the deflecting medium, where $\sigma_j=\left(1+i\right)a_j, a_j=\left(c_j\rho_j\omega_j/2k_j\right), j=1,2,m,b;$ Subscripts 1, 2, m and b refer, respectively, to sample top layer (the layer close to probe laser beam), the bottom layer, the deflecting medium and backing material. ρj the densities, cj the specific heats, kj the thermal conductivities, w is the modulation frequency in rad/s.

One dimensional Theoretical model for photothermal signal generation from semiconductors

Earlier only thermal diffusivity of semiconductors was measured, using signal amplitude as function of modulation frequency. Fournier et al extended this approach of photothermal deflection technique to probe transport properties of semiconductors, such as the thermal

ISSN: 2235-767X
Volume 07 Issue 04
April 2019

diffusivity, the electronic diffusivity, the excess carrier lifetime, and surface recombination velocity. It is an extension of the photothermal deflection technique mentioned above (Sec 1.2) and has advantages that it yields both thermal and electronic transport parameters within the bulk of a semiconductor and also at the surface or at an interface.

An intensity modulated light beam generates a periodic thermal wave due to the optical heating, and in the case of semiconductors the incident light also generates a photo excited carrier population. The thermal wave will propagate into the solid according to usual diffusion process creating a thermal gradient. The photo excited minority carriers will also diffuse away from the surface layer where they are generated and set up population gradient determined by the electronic diffusion, the recombination kinetics (ie., lifetime), and the surface recombination. The recombining carriers will further influence the thermal gradient. Both the thermal gradient and the free carrier gradient will induce a change in the local index of refraction of the solid, which can be probed in situ by the deflection of a probe beam propagating through the fluid adjacent to surface of the solid. Since the changes in the index of refraction are directly related to various transport properties, (namely the thermal and electronic diffusivities, the minority carrier lifetime, and the surface recombination velocity), these parameters can be determined from the dependence of the deflection on modulation frequency.

A one-dimensional theory, which predicts deflection amplitude and phase, allowing the measurement of the transport parameters is demonstrated. A one-dimensional treatment is sufficient since in this case the pump beam, whose dimensions are much larger than both the thermal diffusion and carrier diffusion lengths, uniformly illuminates the front face. In addition, the probe beam is focused and centered well away from the adjoining sides. In order to calculate the resulting deflection, it is necessary to determine the temperature distribution and the carrier distribution throughout the solid. Time dependent deflection of narrow probe beam propagating through an inhomogeneous medium at depth x is given by,

$$\Theta(x,t) = \frac{1}{n}\frac{\delta n(x,t)}{\delta x} \quad \text{.....(1.3)}$$

Where Θ is the angular deflection, *l* is the interaction length (*l* >x, and also much larger than both thermal and carrier diffusion lengths), n is the local index of refraction, and dn (x,t)/dx is the photoinduced gradient in the index of refraction. In the case of semiconductors, dn (x,t)/dx has two contributions, one is thermal and other is free carrier term. This is given by,

$$\frac{\delta n(x,t)}{\delta x} = \frac{\delta n}{\delta T}\frac{\delta T(x,t)}{\delta x} + \frac{\delta n}{\delta N}\frac{\delta N(x,t)}{\delta x} \quad \text{.....(1.4)}$$

Where T (x,t) and N(x,t) are time dependent temperature and the minority carrier density distribution, respectively.

One dimensional Theoretical model for photothermal wave generation and propagation in semiconductor thin films

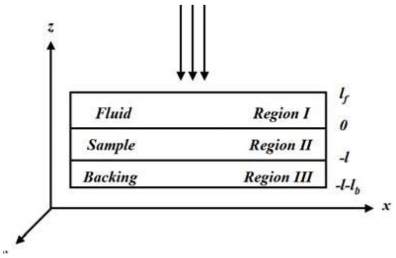

Figure 1.2 Three-layer sample geometry (backing-sample-fluid)

Theoretical model for photothermal analysis of semiconductor put forth by U Zammit et al [10] does not include non-radiative recombination and surface recombination processes taking place in the semiconductors and the model given by Fournier et al [9] does not suit the three layer sample geometry with fluid, sample and backing layer; hence the present model was extended to suit the transverse photothermal beam deflection technique with three-layer sample geometry, assuming the sample to be a semiconductor thin film.

Accuracy of the measurement technique can be improved by further refinement of the theoretical model. We applied this technique for simultaneous measurement of minority carrier lifetime, surface recombination velocity and thermal diffusivity of semiconductor thin films. This technique has further scope for improvement as it can be extended into large area applications as well.

Let us consider the three-layer sample model geometry as shown in figure 1.2. The sample under investigation is irradiated with an intensity modulated laser beam with angular frequency ωmod = 2□f, where f is the modulation frequency. Intensity of the laser beam is given by,

$$I = \frac{I_0}{2} e^{-\beta z} \operatorname{Re}\left[1 + e^{iax}\right] \text{..................................(1.5)}$$

Where I0 is the incident monochromatic light flux (W/m^2), β is the absorption coefficient (m^{-1}) of the illuminated sample and t is the time. It is assumed that the excitation beam energy E = hν, is greater than the band gap of the material, where 'h' is Planck's constant and 'ν ' is the frequency of the beam.

1.3 HEAT DIFFUSION EQUATIONS

The light absorbed by a sample is converted by part or whole into heat by non-radiative de-excitation processes in the material. Thermal conduction is a diffusive process by which the generated heat is transferred from point of origin to other parts of the sample and its surroundings as a result of temperature gradient. Heat conduction is a diffusive process governed by a parabolic differential equation, which lacks second derivative with respect to time. From Fourier's law for heat conduction, the heat flux is proportional to negative of local temperature gradient.

$$q = -kA \frac{dT(z,t)}{dz} \text{..(1.6)}$$

The continuity equation is given by, $\rho c \frac{dT(z,t)}{dt} = -\frac{dq}{dz}$ ....(1.7)

Where k is the thermal conductivity (W/mK), T (z, t) is the temperature, ρ is the density (kg/m3) and c is the specific heat (J/kg K), space coordinate z and time t.

European Journal of Business & Social Sciences
Available at https://ejbss.org/
ISSN: 2235-767X
Volume 07 Issue 04
April 2019

The heat diffusion equation in one-dimensional form, when there is no heat source and sink is given by,

$$\frac{\delta T(z,t)}{\delta t} = \frac{1}{D_S}\frac{\delta^2 T(z,t)}{\delta z^2} \quad \ldots\ldots\ldots\ldots\ldots\ldots\ldots\ldots\ldots\ldots\ldots\ldots\ldots\ldots\ldots\ldots\ldots\ldots(1.8)$$

Where T (z, t) is the temperature, Ds is the thermal diffusivity $\frac{k}{\rho c}\left(\frac{cm^2}{s}\right)$

A semiconductor thin film absorbs the photons with energy greater than the band gap [E_g] of the material, resulting in excess carrier distribution within the semiconductor with energy above (below) the conduction (valence) band. In a time scale of few pico seconds, these photo-injected carriers distribute the energy within themselves through coulomb interaction and finally this extra energy is given to lattice by relaxing to the bottom of the conduction band via carrier phonon interaction. As the excess carriers diffuse through the sample the electron hole pairs will eventually recombine producing a second source of Theoretical background heat. This will also diffuse into the semiconductor. The heat diffusion equation including the heat sources is given by,

$$\frac{\delta T(z,t)}{\delta t} = \frac{1}{Ds}\frac{\delta^2 T(z,t)}{\delta z^2} + q(z,t) \quad \ldots\ldots\ldots\ldots\ldots\ldots\ldots\ldots\ldots\ldots\ldots\ldots(1.9)$$

The three major heat sources are defined by Q (z, t), the net heat power density, are i. Non-radiative intra-band thermalization: When photo generated carriers relax down to the bottom of the conduction band by creating phonons, the heat power density is given by,

$$Q_T(z,t) = \beta\frac{(h\upsilon - E_g)}{h\upsilon} I_0 e - \beta z\left(1 + e^{iax}\right) \quad \ldots\ldots\ldots\ldots\ldots..(1.10)$$

ii. Nonradiative bulk recombination: Non-radiative recombination of excess electron hole pairs after diffusion occurs through a distance (ÖDn t r) where Dn is the carrier diffusivity (m^2/s) and tr (s) is the carrier lifetime. The heat power density due to non-radiative recombination is given by,

$$Q_{NR} = \frac{E_g}{\tau_r} N(z,t) \quad \ldots\ldots\ldots\ldots\ldots\ldots\ldots\ldots\ldots\ldots\ldots\ldots\ldots\ldots\ldots\ldots\ldots\ldots\ldots\ldots\ldots\ldots(1.11)$$

Where N (z, t) is the density of photo carriers, t r is the nonradiative recombination time.
Therefore the total power density is given by, $Q = Q_T + Q_{NR}$
iii. Non-radiative surface recombination: When non-radiative recombination takes place at surface, a heat power density is, $Q_{SR} = E_g V_{sr} N(z, t)$
This thermal contribution has to be included in the boundary condition of heat diffusion equations.

1.3.1 MINORITY CARRIER DIFFUSION EQUATION

When a beam of light irradiates the sample of thickness L, it leads to photo carrier generation; the excess carriers generated can be calculated from minority carrier diffusion.
The continuity equation can be written as,

$$\frac{dn}{dt} = \left.\frac{dN}{dt}\right|_{diffusion} + \left.\frac{dN}{dt}\right|_{drift} + \left.\frac{dN}{dt}\right|_{rec-gen} + \left.\frac{dN}{dt}\right|_{other\ \ process\, like\ light...} \ldots\ldots\ldots(1.13)$$

Where 'N' is the minority carrier concentration. Hence the drift term can be omitted as we consider only low-level injection.

$$\frac{dn}{dt} = \left.\frac{dN}{dt}\right|_{diffusion} + \left.\frac{dN}{dt}\right|_{rec-gen} + \left.\frac{dN}{dt}\right|_{other\ \ process\, like\ light...}$$

For photo-generated carriers the transport equation is given by,

$$\frac{dN(z,t)}{dt} = D_n \frac{d^2N(z,t)}{dz^2} - \frac{\Delta N}{\tau_r} + G(z,t) \ldots\ldots(1.14)$$

Where G (z, t) is the generation rate carriers,

$$G(z,t) = \frac{\beta I_0}{2hv} e^{-\beta z} \ldots\ldots(1.15)$$

To evaluate the excess charge carrier distribution, we make the following assumptions:

i) When the material is in steady state $\frac{dN(z,t)}{dt} = 0$

ii) Since absorption takes place throughout the material thickness, excess carriers are created throughout the material and there is no carrier diffusion along the z direction.

Hence the minority carrier diffusion equation can be written as,

$$\frac{\Delta N}{\tau r} = G(z,t)$$

$$\frac{\Delta N}{\tau r} = \frac{\beta I_0}{2hv} e^{-\beta z} \ldots\ldots(1.16)$$

The heat diffusion equation in the three regions, fluid, sample and backing is,

$$\frac{\delta^2 T_f(z,t)}{\delta z^2} = \frac{1}{D_f}\frac{\delta T_f}{\delta t}$$

$$\frac{\delta^2 T_s(z,t)}{\delta z^2} = \frac{1}{Ds}\frac{\delta T_s}{\delta t} - Q_T - Q_{NR} = \frac{1}{Ds}\frac{\delta T_s}{\delta t} - \beta \frac{(hv - E_g)}{hv} I_0 e^{-\beta z\left(1+e^{iax}\right)} - \frac{E_g}{\tau_r} N(z,t) \ldots(1.17)$$

$$\frac{\delta^2 T_b(z,t)}{\delta z^2} = \frac{1}{D_b}\frac{\delta T_b}{\delta t}$$

One of the boundary conditions is the continuity of temperature at the region boundaries

European Journal of Business & Social Sciences
Available at https://ejbss.org/
ISSN: 2235-767X
Volume 07 Issue 04
April 2019

$$T_f(z,t)\Big|_{z=0} = T_S(z,t)\Big|_{z=0}$$
$$T_S(z,t)\Big|_{z=-l} = T_b(z,t)\Big|_{z=-l} \quad \ldots\ldots\ldots\ldots\ldots\ldots\ldots\ldots\ldots\ldots\ldots\ldots\ldots\ldots\ldots\ldots\ldots\ldots\ldots\ldots\ldots\ldots(1.18)$$
$$T_f(z,t)\Big|_{z=+\infty} = T_S(z,t)\Big|_{z=-\infty}$$

The next boundary condition is obtained from the heat continuity equation, which states that the heat flux flowing out of one region must be equal to heat entering into the adjoining region, must be obeyed.

$$-k_S \frac{\delta T_S(z,t)}{\delta z}\Big|_{z=0} = -k_f \frac{\delta T_f(z,t)}{\delta z}\Big|_{z=0} + V_{sr}\Delta N E_g \quad \ldots\ldots\ldots\ldots\ldots\ldots\ldots\ldots\ldots\ldots\ldots\ldots\ldots\ldots\ldots\ldots\ldots\ldots\ldots\ldots\ldots\ldots(1.19)$$
$$-k_b \frac{\delta T_b(z,t)}{\delta z}\Big|_{z=-l} = -k_f \frac{\delta T_S(z,t)}{\delta z}\Big|_{z=-l}$$

Where ki, Di with i =f, s, b, represents the thermal conductivity and thermal diffusivity of fluid (f), sample (s) and backing (b) respectively.

On solving the thermal diffusion equation (1.17) with boundary conditions (1.18) and (1.19), we get the following expression for complex amplitude of temperature T (z, t) in the three regions.

$$T_f(z) = T_S e^{-\sigma f z}$$
$$T_S(z) = C_1 e^{-\sigma_S z} + C_2 e^{-\sigma_S z} - \left(C_3 + C_4\right) e^{-\sigma_S z} \quad \ldots\ldots\ldots\ldots\ldots\ldots\ldots\ldots\ldots\ldots\ldots\ldots\ldots\ldots\ldots\ldots\ldots\ldots\ldots\ldots\ldots\ldots(1.20)$$
$$T_b(z) = W e^{\sigma_b\left(z+l\right)}$$

Where,

$$C_3 = \frac{\beta l_0}{2k_S}\left(\frac{E-E_0}{E}\right)e^{-\beta z}$$
$$C_4 = \frac{E_g}{\tau_r k_S}\frac{\beta l_0}{2h\nu}e^{-\beta z} \quad \ldots\ldots\ldots\ldots\ldots\ldots\ldots\ldots\ldots\ldots\ldots\ldots\ldots\ldots\ldots\ldots\ldots\ldots\ldots\ldots\ldots\ldots\ldots\ldots\ldots\ldots\ldots\ldots(1.21)$$
$$\sigma_i = \sqrt{\frac{i\omega}{D_i}}$$

The coefficients C_1, C_2 and W were obtained using the boundary conditions. Using C_1, C_2, C_3, and C_4 in equation 3.44, we finally obtain the surface temperature distribution is given by the equation 3.46.

European Journal of Business & Social Sciences
Available at https://ejbss.org/
ISSN: 2235-767X
Volume 07 Issue 04
April 2019

$$T_S = \left\{ \frac{\left[\sqrt{D_f D_S} \left(\begin{array}{l} -R_1 B\sigma_b^2 D_b^{\frac{3}{2}} k_S + R_2 D_S \left\{ \begin{array}{l} B\sqrt{D_S k_b}\left\langle B\beta + Ck_S \right\rangle - \\ \sigma_S \left\langle B\sigma_b \sqrt{D_b k_b} - C\sqrt{D_b k_S^2} \right\rangle \end{array} \right\} + \\ D_S k_S \left(R_3 C\left\{ \sigma_S \sqrt{D_S k_b} + k_S \beta \sqrt{D_b} \right\} + R_1 B\beta^2 \sqrt{Db} \right) \end{array} \right) \right]}{\left[\sqrt{i\omega}\left(i\omega - \beta^2 D_S \right) \left(\begin{array}{l} R_2 \left\{ D_S k_b k_f + \sqrt{D_b D_f k_S^2} \right\} + \\ R_1 \left\{ \sqrt{D_S k_S} \left\langle \sqrt{D_f k_b} + \sqrt{D_b k_f} \right\rangle \right\} \end{array} \right) \right]} \right\} \quad \text{.....(1.22)}$$

where,

$$R_1 \to 1 + e^{2l\sigma_S}$$

$$R_2 \to -1 + e^{2/\sigma_S}$$

$$R_3 \to R_1 - 2e^{l(\beta+\sigma_S)} \quad \text{.....(1.23)}$$

$$B \to V_{sr} N(0) E_g$$

$$C \to C_3 = C_4$$

1.3.2 PHOTOTHERMAL BEAM DEFLECTION SIGNAL

Refractive index gradient in the medium, surrounding the sample, due to heat generated from the sample is given by,

$$\frac{dn}{dz} = \frac{dn}{dT}\frac{dT(z,t)}{dz} \quad \text{.....(1.24)}$$

The deflection of probe beam (signal) thus produced is proportional to the refractive index gradient,

$$\text{signal} \ \alpha \frac{1}{n_0}\frac{dn}{dT}\frac{dT(z,t)}{dz} \quad \text{.....(1.25)}$$

1.4 DETERMINATION OF THERMAL DIFFUSIVITY, MINORITY CARRIER LIFETIME AND SURFACE RECOMBINATION VELOCITY

The parameters thermal diffusivity (Ds), minority carrier lifetime (t r) and surface recombination velocity (Vsr) are to be obtained as 'variable multiple fit parameters' by fitting the experimentally and theoretically obtained plot of modulation frequency versus signal amplitude. The experiment was performed first on silicon wafer and there was good agreement with the experimental data. Transport parameters Ds, t r, Vsr thus obtained were matching with earlier reported values.

European Journal of Business & Social Sciences
Available at https://ejbss.org/
ISSN: 2235-767X
Volume 07 Issue 04
April 2019

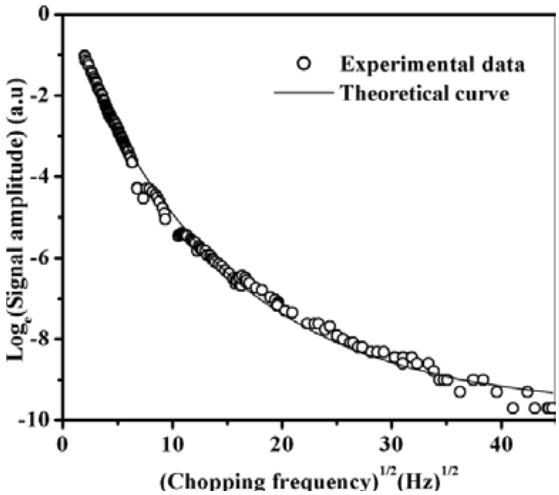

Figure 1.3 Experimental and theoretical fit for semiconductor thin film

1.5 RESULT AND DISCUSSION

1.6 PHOTOTHERMAL STUDIES DONE OVER SILICON WAFER

Further for proving the reliability of theory and technique, photothermal beam deflection studies were done on p-type Si wafer (Figure 1.2). Thickness of the wafer was 300-µm and the optical absorption coefficient was 10^3 cm^{-1} for 632 nm. The optical penetration depth is $1/\beta \sim 3\mu m$ only. Hence the entire incident light is absorbed within the 3- µm distance itself. The deflection signal was higher when the excitation intensity was increased (Figure 1.3).

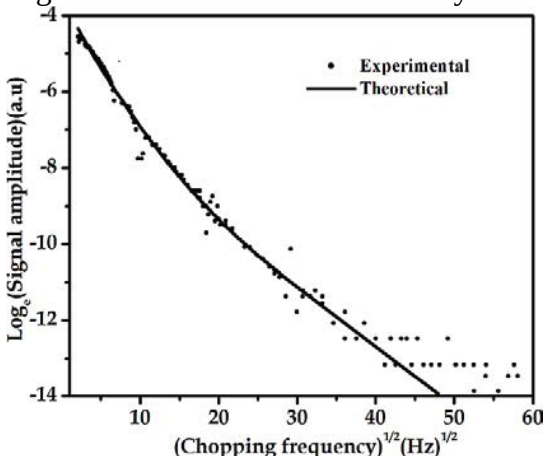

Figure 1.4 Theoretical and experimental plot of photothermal signal for Si wafer

Figure 1.4 shows the theoretical and experimental plot Loge (signal amplitude) Vs (chopping frequency) 1/2 for silicon wafer. It is clear that there is good agreement between the experimental and theoretical curves. Keeping the transport properties D_s, τ_r and V_{sr} as 'variable fit parameters', theoretical fitting was done. Further the Ds ($0.92x10^{-4}$ m^2/s), Zr (30 µs) and V_{sr} (1 m/s) match well with the earlier reports.

1.7 COPPER INDIUM DISULPHIDE

European Journal of Business & Social Sciences
Available at https://ejbss.org/
ISSN: 2235-767X
Volume 07 Issue 04
April 2019

I–III–VI chalcopyrite materials are reported to have very desirable properties for photovoltaic application.(4.2) belonging to this group of compound semiconductor is a promising absorber layer material with optimum optoelectronic properties; cells of this material have already reported efficiencies as high as 12.5% [1] in laboratory scale and 10.2% in industry level [2].

$CuInS_2$ meets the requirements for PV technology with a band gap of 1.5 eV, high absorption coefficient and good stability [3] that suits both terrestrial and space applications [4]. A theoretical calculation by Meese et al (1975) predicted solar conversion efficiencies between 27% and 32% for $CuInS_2$ based homo-junction having a direct band gap of 1.55 eV [5]. Table 1.2 shows the optoelectronic and transport properties of this $CuInS_2$ thin films as reported by other groups. But there are very few reports on the D_S, τ_r, V_{sr} and μ of $CuInS_2$ thin films due to dearth of techniques that are simple and efficient in measuring the transport properties of thin films. The practical difficulties of making such measurements have affected extensive analysis of these properties, which are most essential for fabrication of devices.

TABLE 1.2 : Optoelectronic and transport properties of $CuInS_2$ absorber film

Band gap	1.3 – 1.55 eV [16]
Absorption coefficient	10^5-10^6/cm [16]
Mobility	1-10 cm^2/Vs [6, 17]
Surface recombination velocity	1.2x10^5 cm/s [18]
Carrier concentration	2x10^{18} cm^{-3} [19]
Carrier life time	1.2×10^{-5}s [18]
Resistivity	10^3 to 10^{-1} Ω cm [20, 21]

1.8 PHOTOTHERMAL ANALYSIS OF $CuInS_2$ THIN FILMS

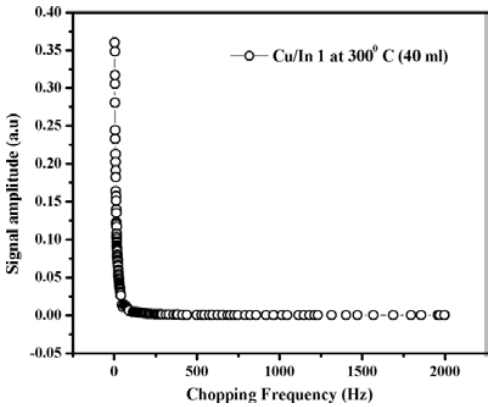

Figure 1.5 Plot of signal amplitude versus chopping frequency for $CuInS_2$ thin films.

Thin films of $CuInS_2$ were excited using the intensity-modulated beam of wavelength 632 nm and the deflection of probe beam was detected using a bi-cell PSD. Figure 1.5 shows the plot

European Journal of Business & Social Sciences
Available at https://ejbss.org/
ISSN: 2235-767X
Volume 07 Issue 04
April 2019

indicating the variation of the amplitude of the deflection of the signal (i.e. probe beam) with respect to the modulation frequency. A Plot of Log_e (Signal amplitude) versus (chopping frequency) $^{1/2}$ (Figure 1.5) clearly shows dependence of signal on frequency. The general trend observed for $CuInS_2$ films, irrespective of the fabrication condition, is the rapid decrease in signal with frequency in the low frequency regime (§ 100 Hz) and gradual or more "slow" decrease in the high frequency regime (¥ 100 Hz). Nature of dependence of signal amplitude on the chopping frequency and the frequency from which the change of slope (showing the 'rapid' or 'slow' decrease) alters with changes in the composition and surface morphology of the investigated film assist us in finding out the origin of non-radiative processes in the film. This can be correlated to the fabrication process and hence useful for optimisation of fabrication process. In the present work, we have made a study on the impact of alternations in film fabrication condition on the transport properties of film.

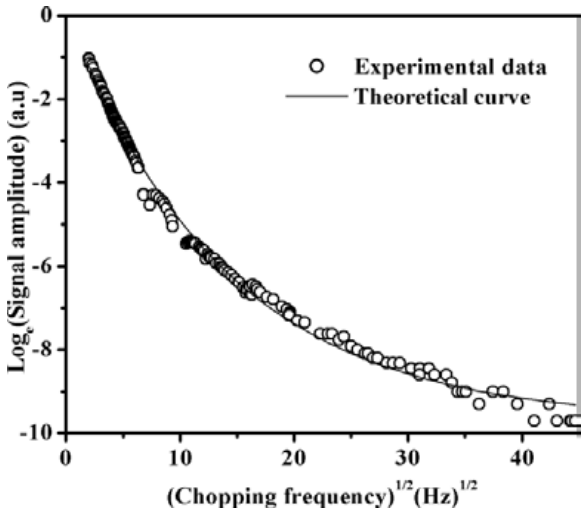

Figure 1.6 Plot of Log_e (signal amplitude) versus (chopping frequency)$^{1/2}$

1.8.1 INFLUENCE OF SUBSTRATE TEMPERATURE

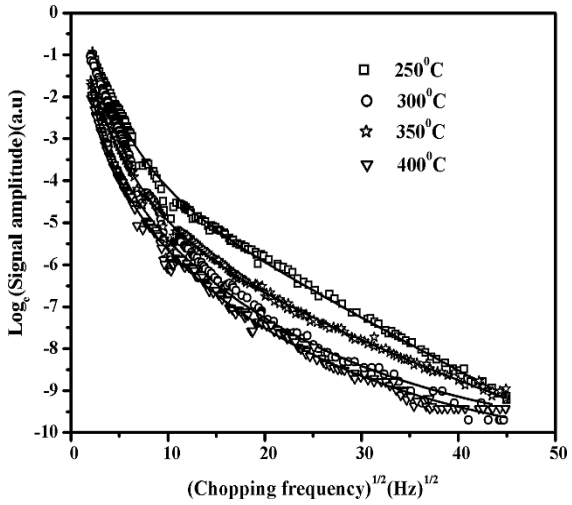

European Journal of Business & Social Sciences
Available at https://ejbss.org/
ISSN: 2235-767X
Volume 07 Issue 04
April 2019

Figure 1.7 Photothermal response of $CuInS_2$ films deposited at 250°C, 300°C, 350 °C, 400°C

Figure 1.6 shows the dependence of the photothermal signal (plot of Log_e (Signal amplitude) versus (chopping frequency) $^{1/2}$) for $CuInS_2$ thin films prepared at different substrate temperatures 250°C, 300°C, 350°C and 400°C. X-ray diffraction studies were done using Rigaku (D Max C) X-Ray diffractometer employing CuK_α line (λ=1.5405 A). From the XRD pattern (Figure 4.6) of this film we could find that, for higher substrate temperature (> 300°C), the crystallinity of the films has improved while for lower deposition temperature (< 300°C) the films had poor crystallinity. We observe that there is no significant variation in the nature of photothermal signal plot except for a slight increase in the deflection signal amplitude for lower substrate temperature (250°C). This suggests that for films prepared at this temperature the non-radiative emission is higher. One of the reasons for having increased non-radiative emission is the presence of surface states and defects in the material, which act as traps with continuum energy states. Electron-hole recombination takes place through this continuum of states with release of phonons that result in photothermal signal generation. D_s, V_{sr}, τ_r determined from the fitting of theoretical and experimental data curve is shown in Table 4.3.

Table 1.3 : Fit data obtained for CuInS2 thin films prepared at different substrate temperature.

Sample °C	Thickness (μm)	Ds ($\times 10^{-3}$ cm^2/s)	τr (ns)	V_{sr} (x 10^8 cm/s)	R (cm^2/Vs)
250	0.51	0.85	20	5	0.40
300	0.46	0.85	350	2	0.50
350	0.35	0.88	50	8	0.30
400	0.27	0.88	40	10	1.59

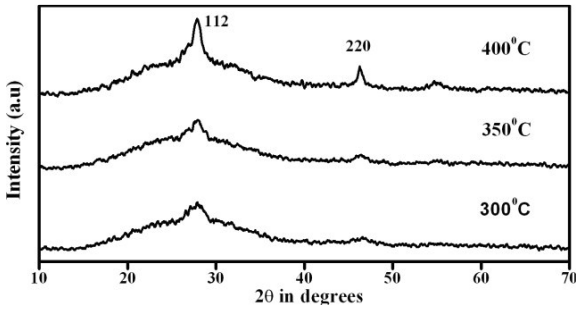

Figure 1.8 XRD patterns of samples deposited at substrate temperature 300°C, 350°C and 400°C

This also suggests that 300°C is comparatively the best temperature suited for preparation of $CuInS_2$ films using CSP technique, as it offers very high τ_r. Also the non-radiative emission at this temperature is the least; this indicates better films with low recombination losses. So the substrate temperature plays a critical role in deciding the transport properties of the

European Journal of Business & Social Sciences
Available at https://ejbss.org/
ISSN: 2235-767X
Volume 07 Issue 04
April 2019

fabricated film. The formation of defects and deformities can be reduced to certain extend by choosing the optimum deposition temperature.

1.8.2 INFLUENCE OF FILM COMPOSITION

Concentration of copper and indium in the spray solution has to be controlled. The excess or deficiency of the "metal" (Cu & In) in the film would alter the film's properties. So it is essential to choose the concentration of constituents in the film in accordance with device requirements. For the present study, films were prepared by varying the ratio Cu/In as 0.5, 1 and 1.5, and figure 1.8 shows variations in the photothermal signal plot for different Cu/In in the film. Transport properties determined from the theoretical best-fit show that V_{sr} is very high for Cu deficient samples, while for Cu rich (Cu/In ~1.5) samples, V_{sr} reduced by 10^4 times. These values were in good agreement with reported values [18, 23]. Also the crystallinity is better for Cu rich films (Figure 1.9). Surface morphology is much better when there is Cu excess in the film. The AFM images of Cu rich (Figure 1.10 a) and Cu-deficient films (Figure b) also support the conclusions from photothermal analysis. For stoichiometric films (Cu/In ~ 1), carrier lifetime was the highest and mobility was the highest and mobility was also higher compared to Cu rich and Cu poor films (Table 1.4). Hence the stoichemic films are best suited for device fabrication.

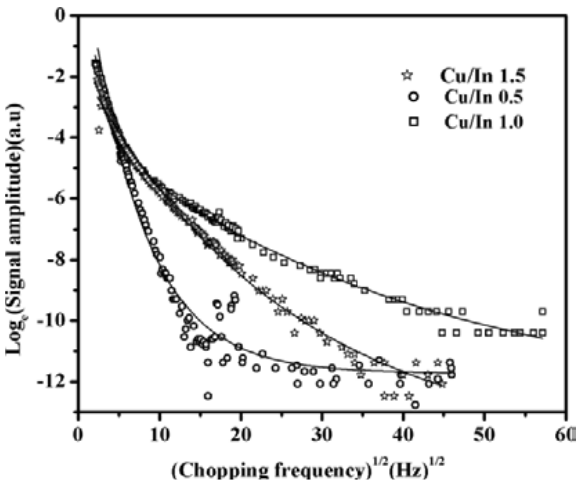

Figure 1.9 a Photothermal response of $CuInS_2$ films with Cu/In 0.5, 1, 1.5

European Journal of Business & Social Sciences
Available at https://ejbss.org/
ISSN: 2235-767X
Volume 07 Issue 04
April 2019

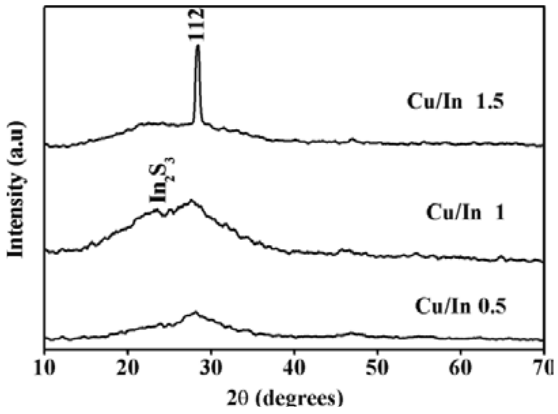

Figure 1.9 b XRD patterns of $CuInS_2$ samples with Cu/In 0.5, 1, 1.5

Table 1.4

Sample (Cu/In)	Thickness (μm)	Ds (x $10^{-3}cm^2/s$)	τr (ns)	Vsr (x $10^5cm/s$)	R (cm^2/Vs)
0.5	0.58	0.79	10	13×10^4	0.23
1.0	0.46	0.85	350	2×10^5	0.80
1.5	0.25	1.90	1	5	0.21

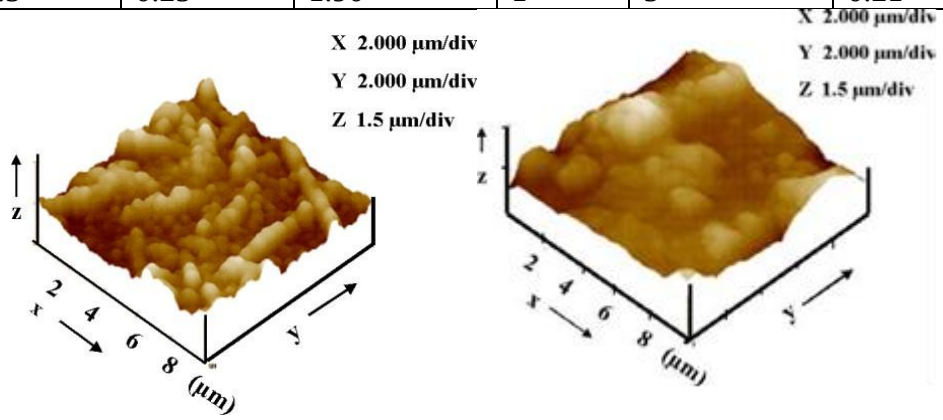

Figure 1.10 2-D AFM image (a) Cu rich (b) Cu deficient

1.8.3 INFLUENCE OF SPRAY VOLUME

Figure 1.10 show that variation in spray volume slightly altered the non-radiative nature of the films. But the crystallinity improved with increase in volume of spray solution (Figure 1.11). Value of V_{sr} was highest for 20 ml spray volume since the film formation is rather incomplete when spray volume in less than 30 ml; hence the formation of surface states is higher, resulting in high non-radiative loss, in this case. While for spray volume 30 ml and 40 ml, V_{sr} is the least and lifetime is slightly better for films with 30 ml spray volume. Films fabricated with 40 ml spray solution exhibited good crystallinity (Figure 1.11).

European Journal of Business & Social Sciences
Available at https://ejbss.org/
ISSN: 2235-767X
Volume 07 Issue 04
April 2019

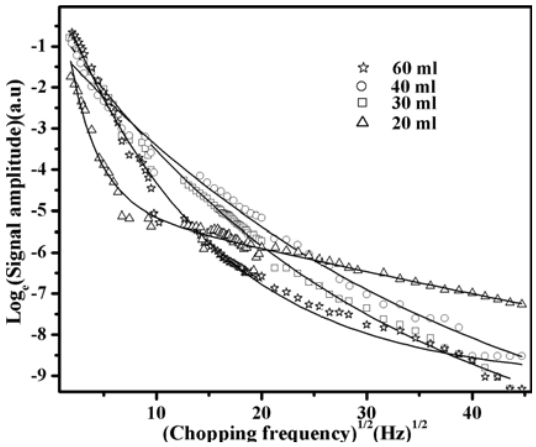

Figure 1.11 Photothermal response of $CuInS_2$ films with spray volume 20, 30, 40 and 60 ml

However D_s was higher for 30 ml sample (Table 1.5). Hence from these results, one can conclude that it is better to choose spray volume at 30 ml as optimum spray volume for fabrication of good quality solar cell absorber layer, since at this spray volume, the film has high D_s ($4.8x10^{-3}$ cm^2/s), high τ_r (4 ns), low V_{sr} ($5 x10^5$ cm/s) and high μ (0.30 cm^2/Vs).

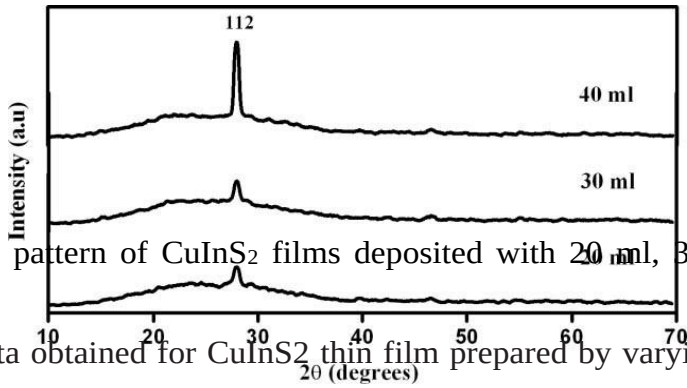

Figure 1.12 XRD pattern of $CuInS_2$ films deposited with 20 ml, 30 ml, 40 ml spray volume

Table 1.5 : Fit data obtained for CuInS2 thin film prepared by varying the spray volume

Sample (Cu/In)	Thickness (μm)	Ds (x $10^{-3}cm^2/s$)	τr (ns)	Vsr (x 10^5cm/s)	R (cm^2/Vs)
0.5	0.58	0.79	10	13×10^4	0.23
1.0	0.46	0.85	350	2×10^5	0.80
1.5	0.25	1.90	1	5	0.21

European Journal of Business & Social Sciences
Available at https://ejbss.org/
ISSN: 2235-767X
Volume 07 Issue 04
April 2019

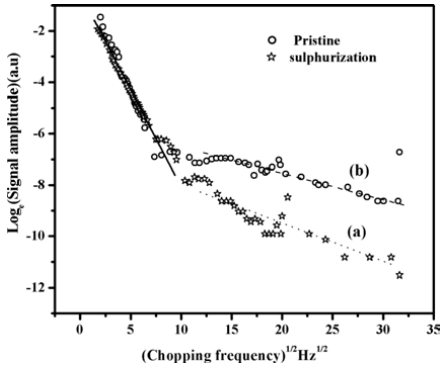

Figure 1.13 : Photothermal response of $CuInS_2$ films with and without post deposition H_2S treatment

Table 1.6 : Fit Data obtained for $CuInS_2$ thin film prepared by varying the spray volume

Sample	Thickness (μm)	Ds ($\times 10^{-3}$ cm^2/s)	τ_r (ns)	V_{sr} ($\times 10^5$ cm/s)	(cm^2/V_s)
20 ml	0.13	0.73	0.7	50	0.025
30 ml	0.17	4.8	4.0	5	0.30
40 ml	0.25	1.9	1.0	5	0.16
60 ml	0.33	1.7	0.3	10	0.056

1.8.3 INFLUENCE OF H_2S TREATMENT ON $CUINS_2$ THIN FILMS

Non-radiative response of 'sulphurized' and 'unsulphurized' sample is shown in figure 1.12. We observed that the non-radiative recombination loss is lower for sulphurized samples. These samples (sulphurized) have better transport properties too. V_{sr} reduced by one order ($7x10^4$ cm/s); τ_r has also increased considerably (2 μs)(Table 1.6). Figures 1.13 and 4.14 show the J-V plot of $Ag/In_2S_3/CuInS_2/ITO$ cells CIS (Without H_2S treatment) and CIS-S (with H_2S treatment). It is known that μ plays a major role in determining the cell's open circuit voltage through its effect on saturation current. As a result, the 'sulphurized' sample shows no shift on illumination inspite of better V_{sr} and τ_r. This is because the sulphurized samples have comparatively low mobility (0.37 cm^2/Vs) while for untreated samples μ is higher by one order (1.2 cm^2/Vs).

European Journal of Business & Social Sciences
Available at https://ejbss.org/
ISSN: 2235-767X
Volume 07 Issue 04
April 2019

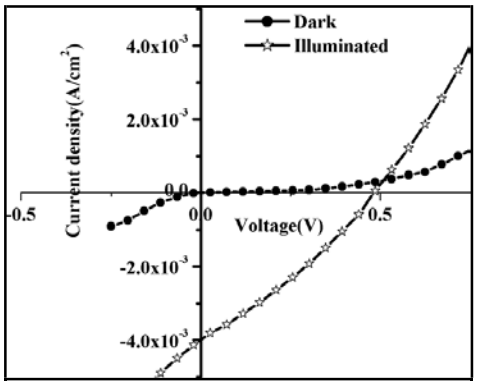

Figure 1.14 J-V Plot of $CuInS_2/In_2S_3$ cell cell without H_2S treatment

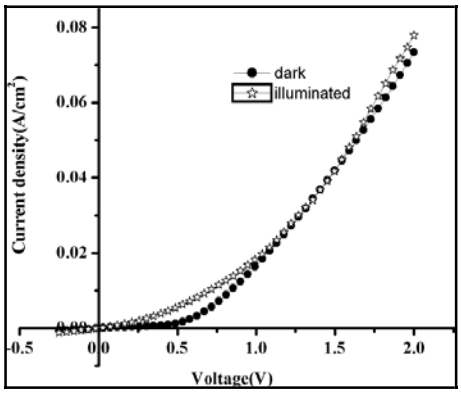

Figure 1.15 J-V Plot of $CuInS_2/In_2S_3$ with H_2S treatment

Table 1.7 : Transport properties of $CuInS_2$ films with and without H_2S treatment

H_2S Treatment	Ds (cm^2/s)	2r (s)	Vsr (cm/s)	μ (cm^2/Vs)
Without	0.8×10^{-7}	0.8×10^{-6}	1×10^{5}	1.2
With	1.6×10^{-7}	2×10^{-6}	0.7×10^{5}	0.37

Earlier reports also advocate that for sprayed $CuInS_2$ films H_2S treatment results in significant improvement of structural and optical properties while conductivity and concentration of carriers decreased [20]. This may be due to the 'scavenging' of Cu atoms in $CuInS_2$ films through Sulphur annealing [25] and heavy compensation of the intrinsic defects in the material. As a result, the number of holes (majority carriers) reduces considerably. Hence the probability of electron–hole recombination falls resulting in an increase in lifetime of minority carriers. Thus, we observe that an increase in lifetime with increase in number of minority carriers which cause decrease in μ.

1.9 CONCLUSION

We brief the basic theoretical works that form the foundation of development of photothermal technique and helped it grow into a widely accepted and recognized non-destructive material analysis tool. Reliability and accuracy of the theoretical model developed in this work is proven with measurements made on Si wafer. Values of thermal diffusivity, carrier lifetime and recombination velocity thus calculated match very well with earlier reports.

Theoretical model developed for determining the transport properties of semiconductor thin films is simple and can be extended to suit multilayer films also.

PTBD technique was successfully used to measure D_S, μ, τ_r and V_{sr} of $CuInS_2$, $CuInSe_2$ and SnS thin films, which find application as absorber layer in thin photovoltaic devices. The non-radiative nature of films is also analyzed and the results are correlated with other optical, structural and composition analysis tools, to optimize the deposition parameters that yield device quality thin films. Thus, through this work, we could establish the application of PTBD as an efficient and simple tool for real time thin film analysis for controlling the

ISSN: 2235-767X
Volume 07 Issue 04
April 2019

device fabrication process.

REFERENCES

- A Rosencwaig 1973 Opt Comm 7 305
- A C Boccara, D Fournier, W Jackson, N M Amer 1980 Opt Lett 5 377
- J A Sell, D M Heffelfinger, P L G Ventzek, R M Gilenbach 1981 J Appl Phys 3 69
- M Bertolotti, L Fabbri, C Sibilia, A Ferrari, N Sparvier, G Suber 1988 J Phys D: Appl Phys 21 S14
- S D George, P Radhakrishnan, V P N Nampoori, C P G Vallabhan 2003 Phys Rev B 68 165319
- J C Murphy, L C Amodt, 1980 J Appl Phys 51 4580
- H M James 1980 J Appl Phys 51 4666
- J Opsal, A Rosencwaig 1982 J Appl Phys 53 4240
- D Fournier, C Boccara, A Skumanich, N M Amer 1986 J Appl Phys 59 787
- U Zammit, F Gasparrini, M Marinelli, R Pizzoferrato, F Scuderi, S Martellucci 1991 J Appl Phys 69 2577
- S Y Zhang, J C Cheng, 1991 Semicond Sci Technol 6 670
- J C Cheng, S Y Zhang 1991 J Appl Phys 70 7007
- J D Spear, R E Russo 1991 J Appl Phys 70 580
- X Quelin, B Perrin, G Louis, P Peretti 1993 Phys Rev B 48 3677
- P Grunow, R Schieck 1995 J Appl Phys 77 2773
- T T N Lan, H G Walther 1996 J Appl Phys 80 5289
- G G de la Cruz, Y G Gurevich 1996 15th International conference on Thermoelectrics, California 217
- A Mandelis, A Salnick, J Opsal, A Rosencwaig 1998 J Appl Phys 85 1811
- S Galovic, M D Dramicanin 1999 J Phys D Appl Phys 32 1511
- C Glorieux, R Li Voti, J Thoen, M Bertolotti, C Sibilia 1999 Inverse Problems 15 1149
- R Li Voti, C Melchiorri, C Sibilia, M Bertolotti 2001 Anal Sci 17 S410
- R Li Voti, G L Liakhou, S Paoloni, C Sibilia M Bertolotti 2001 Anal Sci 17 S414
- A Salnick, J Opsal 2002 J of Appl Phys 91 2874
- Y G Gurevich, G N Logvinov, G G de la Cruz, G E López 2002 Int J of Therm Sci 42 63
- E Marin, J M Antuna, P D Arencibia 2002 Eur J Phys. 23 523
- J H Zhao, J Shen, C Hu 2002 Opt Lett 27 1755
- Y G Gurevich, G N Logvinov, G G de la Cruz, G E Lopez 2003 Int J of Therm Sci 42 63
- B Li, A Mandelis, Z Z Kish 2004 J of Appl Phys 95 1042
- K Boubaker 2004 Eur Phys J Appl Phys 28 249
- M Soltanolkotabi, M H Naderi 2004 Jpn J Appl Phys 43 611
- G N Logvinov, M C Irisson, I M Lashkevych, J E Velazquez, Y G Gurevich 2006 Brazlian J of Physics 36 1097

ISSN: 2235-767X
Volume 07 Issue 04
April 2019

- R Mulaveesala, S Tuli 2006 Appl Phys Lett 89 191913
- J H Rohling, J Shen, C Wang, J Zhou, C E Gu 2008 Eur Phys J 153 99
- M Paulraj 2004 PhD Thesis, Cochin University of Science and Technology, India